R01 – 93

Penetration Failure Mechanisms of Armor-Grade Fiber Composites under Impact

B. L. LEE*, T. F. WALSH, S. T. WON AND H. M. PATTS
The Pennsylvania State University
Department of Engineering Science and Mechanics
University Park, PA 16802

J. W. SONG
U.S. Army Soldier Systems Command RD&E Center
Science & Technology Directorate
Natick, MA 01760

A. H. MAYER
U.S. Air Force Research Laboratory
Air Vehicles Directorate
Wright-Patterson Air Force Base, OH 45433

(Received January 21, 1999)
(Revised March 27, 2000)

ABSTRACT: The penetration failure mechanisms of "armor-grade" fiber-reinforced composites with very low resin content were assessed under transverse impact loading in comparison with those of dry reinforcing fabrics. Failure of dry fabrics consisted of the successive fracture of individual yarns along the periphery of the penetrating head as well as the movement of yarns slipping off from the penetrator. In contrast, the principal yarns in the composites, which faced the penetrating head, failed to carry the load mostly through fracture due to the constraint of the resin matrix and the reduced yarn mobility. As a result, the composites absorbed more energy than the fabrics. The ratio of the number of broken yarns in the fabrics to that of the composites correlated quite well with the corresponding ratio of energy absorbed, confirming that fiber straining is responsible for most of the energy absorption in penetration failure. Numerical modeling was utilized to show that yarn slippage in the fabrics results in a smaller effective penetrator radius leading to a decrease in energy absorption capacity with equal penetrator masses. Although the resin matrix itself did not absorb significant amounts of energy, it certainly had an indirect effect on the en-

*Author to whom correspondence should be addressed.

0021-9983/01/18 1605–29 $10.00/0 DOI: 10.1106/YRBH-JGT9-U6PT-L555

ergy absorption capacity of composites by influencing the number of yarns broken. Stiffer resin matrix prevented the yarn movement to a greater degree and thereby forced the penetrator to engage and break more yarns. Up to the thickness of 3 mm, the dependence of the kinetic energy for full perforation of composites on the laminate thickness was close to the case of ductile monolithic materials such as polycarbonate or aluminum but in less linear fashion. The deviation from the linearity was attributed to a unique mode of tensile failure of armor-grade composites in which a critical level of kinetic energy for full perforation is lowered by the mobility of yarns.

KEY WORDS: penetration failure, ballistic impact, drop-weight impact, static puncture, fiber-reinforced composites, Spectra® oriented polyethylene fiber, Kevlar KM2® aramid fiber, armor-grade fiber composites.

INTRODUCTION

AS DISCUSSED IN our earlier paper [1], light-weight composite structures for ballistic protection often utilize outstanding impact resistance of high-modulus, high-strength polymeric fibers such as Kevlar® aramid or Spectra® oriented polyethylene fibers [2–6]. These fibers in the form of collimated continuous filaments or woven fabrics are embedded in the resin matrix forming a unique class of structural composites, so-called "ballistic-grade" or "armor-grade" composites. The armor-grade composites are constructed with a very low resin content, around 20% by volume, to achieve maximum utilization of inherently high resistance of fibers to the transverse impact. As a result of very low resin content, these composites are relatively flexible unless a structure of considerable thickness is constructed.

Armor-grade composite laminates prepared from aramid fiber-reinforced phenolic-polyvinylbutyral resin or Spectra fiber-reinforced vinyl ester resin are widely used in hard personnel armor systems, such as protective helmets, against fragments from exploding munitions [6–11]. Increasing use of aramid or Spectra fiber composites for ballistic protection is also found in light-weight armored shelter [5]. Penetration failure resistance of the armor-grade composites can be further increased by attaching the front plate of hard ceramics resulting in hybrid structures. Hybrid structures of fiber composite backing plate and ceramic front plate have been developed for bullet-protective armor systems.

For afore-mentioned applications, the most important parameter in evaluating the ballistic impact resistance of materials is a critical level of projectile velocity or kinetic energy applied to the system (ballistic limit) below which no full perforation occurs [11,12]. Also important are the residual strength and damage tolerance characteristics of the materials with partially penetrated projectiles or surface damages, which determine the long-term survivability of the protective systems. As amply demonstrated by the past investigations, ballistic impact is a highly dynamic event involving transient stress wave propagation [13–17]. In many cases, the impacted material will fail before the stress waves reflect from the material

boundaries [17]. Although the velocity of ballistic impact is much greater than that of low-velocity drop-weight impact, the loading conditions of ballistic impact involve variable penetration velocity, as in drop-weight impact, since the penetrator decelerates during the event.

The current study aims at the establishment of the failure criteria for the armor-grade fiber-reinforced composites with very low resin content under impact loading. The establishment of the failure criteria is to be followed by the efforts for modeling of the damage tolerance of the composites under repeated impact. As a first step toward these goals, penetration failure modes of Spectra polyethylene fiber-reinforced resin composites were examined in detail in our previous investigation [1]. The study revealed that both woven fabric-reinforced and angle-plied fiber-reinforced composite laminates exhibit complex failure processes involving delamination, cut-out of a plug, resin matrix cracking, fiber pullout, and fiber fracture, as observed in the case of conventional structural-grade composites reinforced with glass or carbon fibers. When subjected to the repeated impact of a constant striking velocity below the ballistic limit, a progressive growth of local delamination was observed until full perforation of composites occurred. The use of lower striking velocity of the projectile led to the increase in cumulative numbers of impacts for full perforation defining an impact fatigue lifetime profile.

One interesting finding in the course of investigation was that the resin matrix properties have some influence on the penetration resistance of armor-grade composites despite their very low resin content. For instance, Spectra fabric-reinforced composites with vinyl ester resin matrix have a higher ballistic limit and longer impact fatigue life at a given striking velocity than the polyurethane matrix composites. In our earlier paper [1], less effective absorption of impact energy by flexible polyurethane matrix composites was attributed to much more restrained pattern of delamination growth. Correlated with the results of dynamic mechanical analysis, it was also postulated that the stiffness of resin matrices may play an important role in controlling the ballistic impact resistance of Spectra fiber composites. However, despite the observed effect of resin matrix properties on the ballistic performance, the study done by other investigators [17,18] as well as our study [1] strongly suggests that the dominant energy absorption mechanism of armor-grade composites is fiber straining. Fiber straining as the dominant energy absorption mechanism is discussed in detail in the ensuing section.

Scope of Work

The current investigation plans to resolve these two seemingly conflicting issues and to provide more complete explanation of the effects of resin matrix properties on the penetration failure resistance of armor-grade composites, specifically Spectra polyethylene and Kevlar aramid fabric-reinforced composite laminates with very low resin content. In an effort to gain a fundamental understanding of the

deformation and failure processes involved, the scope of the work has been broadened to include the static puncture resistance and drop-weight impact resistance of single ply plain-weave dry fabrics as well as single-ply fabric-reinforced composite laminae. In order to establish a theoretical basis for yarn slippage phenomena and the corresponding difference in performances between dry fabrics and composite laminae, a numerical model was developed to compute the load-deflection curves under static penetration loading with various penetrator radii. The general trends elucidated in the experimental data were compared to the predictions of the model.

In the case of multi-ply composite laminates, the total amounts of energy absorbed during penetration were measured at strain rates ranging from static to ballistic impact loading. These experiments were performed for the Spectra polyethylene fabric-reinforced composite laminates with vinylester and polyurethane resins as matrices to evaluate the effects of matrix properties on the overall performance and failure modes. Finally, for aramid fabric-reinforced composite laminates, the effects of laminate thickness on the ballistic performance and failure modes of composite structures were examined to further assess the relationship between fiber straining and fiber mobility in controlling energy absorption mechanisms.

REVIEW OF PAST LITERATURE

In the past, numerous experimental and analytical investigations were undertaken to uncover the penetration failure mechanisms of the fiber-reinforced composites versus other armor materials under impact [2–4,19–32]. Some investigations focused on the response of textile fabrics without any resin matrix to ballistic impact [15–18], while others investigated the role of resin matrix properties [1,18]. The effects of the presence of a small amount of resin matrix (20%) on the overall performance of composites have not been fully characterized, particularly with regard to textile fabric reinforcement. Here the complicated decrimping mechanisms are expected to occur during the final stages of penetration failure of woven fabrics and they should be influenced by the effect of yarn-to-yarn coupling due to the presence of a small amount of resin.

In examining the role of resin addition on the impact resistance of textile composites, Hsieh et al. [18] subjected aramid and Spectra dry fabrics and their fabric-reinforced composite laminates to low-velocity as well as ballistic impact. For both aramid and Spectra composites, the composites outperformed their corresponding dry fabric for the entire range of thickness tested. Postmortem examination of the specimens revealed that more fibers were broken in the composites than in the fabrics. Noting a primary role of fiber straining in energy absorption under impact, the observed fact may be used to explain the trend of superior impact performances of composites at least in a qualitative sense.

Dent et al. [17] examined the deformation and perforation behavior of single-ply aramid and nylon dry fabrics by subjecting them to the ballistic impact of hemispherical as well as right circular cylindrical (blunt-nosed) projectiles of 4.15 grams at speeds ranging from 300 to 500 m/s. It was found that most of the yarns lying within the path of the blunt-nosed projectiles were strained to failure, whereas many yarns in the panels impacted with hemispherical projectiles slid off of the projectile due to the surface curvature and were pushed aside without being broken. As a result, the critical velocities for penetration of the panels impacted with blunt-nosed projectiles were about 20% higher than those impacted with hemispherical projectiles.

In the case of multi-ply composite laminates reinforced with collimated Spectra fibers as well as woven Spectra fabrics, the failure modes under the ballistic impact were closely examined in our earlier study using fragment-simulating projectiles of 1.1 grams [1]. At a speed ranging from 150 to 300 m/s, both the angle-plied Spectra 1000® web-reinforced and the Spectra 900® woven fabric-reinforced composite laminates were found to exhibit sequential delamination, cut out of a plug induced by through-the-thickness shear, and combined modes of shear cut-off and tensile failure of fibers. In the angle-plied laminates, the fibers experiencing the initial impact failed in shear or cutting, which seemed to occur at the edge of the projectile. In those cases where fiber damage was visible in the back layers of the laminate, the mode closely resembled tensile failure. However, many of the thin laminates appeared to allow the projectile to penetrate by moving fibers laterally or inducing fiber pull-out rather than straining the fibers to break.

The delamination in the angle-plied Spectra fiber-reinforced composite laminates closely resembled the "generator strip" phenomenon reported by Sierakowski et al. [19] in conventional composites of glass fiber-reinforced epoxy resin. Under impact, the projectile pushed a strip of the first layer of the laminate toward the rear of the panel inducing shear cracks in the resin matrix parallel to the fibers, which applied a transverse load to the second ply and resulted in a separation between the first two laminae. After the successive delamination had spread through the plies of the laminate leading to the perforation, narrow strips of damage zone were still visible under the transmitted light. The axis of damage zone tended to follow the angle of the respective fiber orientation in the panel. Around the perforated area, a circular zone of delamination was clearly visible. The observation indicated that the narrow strips of damage zone consist of matrix/interface cracks between the fibers and the resultant delamination. A considerable degree of fiber pull-out was observed in the thicker panels.

In contrast to the case of angle-plied fiber-reinforced composite laminates, Spectra fabric-reinforced laminates exhibited much less lateral movements of reinforcing fibers during the penetration of the projectile [1]. Even in thin panels, fibers apparently failed due to shear or cutting mode in the plies close to the striking surface and in tension at the rear of a completely penetrated panel. The presence of

a strip of finite width of the first lamina pushed forward by the penetrator could not be observed in the Spectra fabric-reinforced laminates. Instead the delamination zones were observed preferentially along the two reinforcement directions of woven fabric. However, these damage zones were closely integrated with a circular zone of delamination around the perforated area. The occurrence of less anisotropic pattern of delamination was understandable considering the presence of resin-rich pockets between the reinforcing layers as well as a greater constraint to matrix crack propagation parallel to the fibers.

EXPERIMENTS

Materials

The current study utilized the following material systems based on the plain-weave fabric of Spectra® 900 oriented polyethylene: (a) single ply of dry fabric, (b) single ply of fabric-reinforced composite lamina, (c) 5-ply fabric-reinforced composite laminate (~1.5 mm thick), (d) 23-ply fabric-reinforced composite laminate (6.71 mm thick). Two different types of resins, vinyl ester (Dow Derakane® 411-45) and aliphatic ester type polyurethane (Mobay Dispercoll® E-585), were used as matrices for Spectra fabric-reinforced composites. The dry fabrics of Spectra were received from Allied-Signal, Inc. (Petersburg, VA).

In addition to these Spectra fabric-reinforced composites, composite laminates of various thickness were prepared from the material combination consisting of: plain-weave fabric of Kevlar KM2® aramid, and phenolic-polyvinylbutyral 50/50 blend resin (a proprietary resin of Bedford Materials, formerly Westinghouse Electric Corporation, Bedford, PA). A systematic variation of laminate thickness was achieved by stacking 3 to 31 plies of aramid fabric composites with the final average thickness ranging from 0.73 to 7.02 mm. All composite prepreg materials reinforced with either aramid or Spectra fabrics were supplied by Bedford Materials, Inc. The resin contents of final composites were approximately 25% by weight for both systems.

Molding

The composite panels were prepared by pressing prepreg plies between two flat aluminum plates. Relying on a programmable press, the temperature was raised at a constant rate from room temperature to the cure temperature where it remained for a fixed period of time ("cure time"), and was then lowered to room temperature at a constant rate. The pressure was held constant throughout the curing cycle. The respective levels of heating rate, cure temperature, cure time, cooling rate, and pressure were: 11°C/min, 116°C, 20 min, 11°C/min, 3.83 MPa (555 psi) for Spectra fabric composites; 20°C/min, 163°C, 12 min, 30°C/min, 6.895 MPa (1000 psi) for aramid fabric composites. The cured composite panels were then removed from the press at room temperature.

Penetration Testing

Penetration testing was performed under static (0.000254 m/s, screw-type tester), low-velocity impact (3.8 m/s, drop-weight tester) and ballistic impact (100–500 m/s, pressurized helium gas gun) loading conditions along the through-the-thickness direction. Two types of projectiles were used in ballistic tests: (a) fragment-simulating steel projectile (FSP) of 1.1 gram (17 grain) mass and 5.6 mm diameter; (b) tungsten carbide ball of 16 gram mass and 12.7 mm diameter. For static puncture tests and drop-weight impact tests, the shape of the penetrating steel head was a replica of 17-grain FSP, as shown in Figure 1. This penetrator presents a rectangular area as front face to the target initially. The rectangular area is then followed by two inclined planes, which taper into the full penetrator diameter of 5.6 mm. Tungsten carbide ball of 16 gram mass and 12.7 mm diameter was used only for ballistic testing of 23-ply laminates of Spectra fabric composites and 3 to 31-ply laminates of aramid fabric composites.

A proper comparison of the true penetration resistance of different materials would be impossible if the specimen slippage and resulting frictional energy losses occurred during testing. Specimen slippage would also adversely affect the

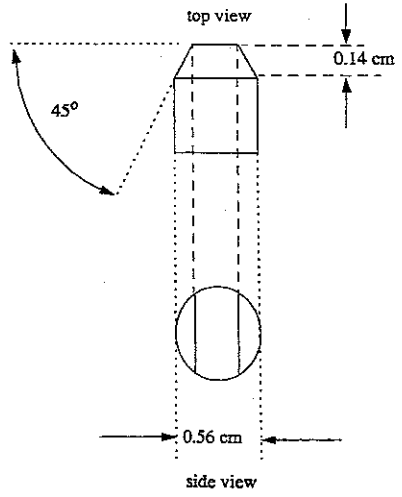

Figure 1. *A fragment-simulating projectile (FSP) used to evaluate the armor system for its effectiveness in arresting ballistic fragments.*

repeatability of the test results. Under impact loading, slippage seldom occurs with rigid plates. As a result, existing impact test standards such as ASTM D3029 [33] and D5420 [34] do not require a specific level of clamping pressure. The pneumatic fixtures provided with typical drop-weight impact testers often allow adequate clamping pressure for testing of rigid composite plates. However, the testing of dry fabric and flexible textile composites with low resin content is highly prone to the slippage of the specimen, since the penetrating head strikes and pulls the target out of the clamping plates much more easily due to the presence of in-plane membrane tension. At present, there is no ASTM standard procedure for impact testing of flexible armor-grade composites.

In the current investigation, a specialized set of flat steel plates with serrated surface was developed to provide a high level of friction between the specimens and the gripping surfaces, as well as high levels of clamping pressure. As shown in Figure 2, the gripping surfaces of the clamping plates consisted of pyramid-shaped serration units repeated in a regular fashion. Such sharp serrated surfaces, along with large clamping forces, were needed to completely eliminate the specimen slippage. For penetration testing of dry fabrics, composite laminae, as well as composite laminates, the specimen was placed between two clamping plates with a 76.2 mm diameter hole (so-called "aperture") in the center. The clamping force was varied by tightening each bolt to a specified torque. The total amount of torque applied to the bolts was varied systematically and the corresponding clamping force was calculated using a simple screw equation.

For ballistic impact testing of composite laminates, the panel was placed between two clamping plates of same serrated surface with 150 mm diameter hole in the center and firmly tightened. The clamping plates with 50 or 100 mm diameter hole were also used in comparison. No significant effect of aperture size on the ballistic resistance was noted, as described in our earlier paper [1]. The striking velocity and residual velocity after perforation were estimated respectively from the time of passage between the light screens connected to an electronic timer. As discussed earlier, the ballistic limit is a critical level of projectile velocity or kinetic energy applied to the system below which no full perforation occurs [11,12]. Accordingly, the ballistic limit velocity, V_{50}, is defined in the current study as the highest striking velocity where the residual velocity equals zero. A series of tests at various levels of striking velocity, which led to either full perforation or no/partial perforation, were performed to estimate the ballistic limit.

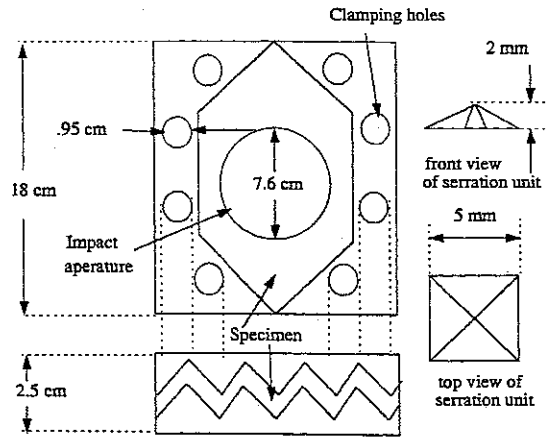

Figure 2. *A clamping fixture for static puncture and low-velocity impact loading.*

Postmortem Inspection

Using optical microscope as well as scanning electron microscope (SEM), dry Spectra polyethylene fabrics and Spectra or aramid fabric-reinforced composite panels were examined after penetration of projectile. Microscopic examination was performed to assist in quantifying the failure region dimensions in terms of the number of broken yarns and to inspect the resulting changes in the weave structure around the perforated area. In order to increase the conductivity, specimens were gold-coated prior to SEM examination.

Since Spectra fabric-reinforced composite laminates were translucent, the study of damage patterns was relatively easy under transmitted light. This technique was used to study the interlaminar damage patterns in multi-ply laminates as well as to assist in determining if sufficient clamping forces were used to prevent specimen slippage. Measurement of the failure region dimensions in terms of the number of broken yarns was carried out in the case of composite laminates after deplying. Deplying of the laminate into the individual plies was done by immersing the panels in toluene for several days.

NUMERICAL MODELING

As an integral part of the research work, a numerical model was developed that simulates the penetration process in a single ply of dry plain-weave fabrics. The model was formulated to perform parametric studies of variables involved in the penetration process of fabric, and to evaluate various constitutive relationships by comparing the predictions of the model with experimental data. In this model, the fabric was idealized as a pin-jointed network of elastic members that support tension only, an approach already taken by several researchers for ballistic impact of textile fabrics [14–16,29]. However, the present model employed a quasi-static so-

lution of the global fabric response. A simple heuristic description of this model is given in the rest of this section. A more detailed discussion is reserved for a future publication.

A particular approach used in the current modeling efforts was chosen due to its ability to provide a realistic description of the fabric structure. It has been well-recognized that conventional continuum models which consider the fabric to be a membrane [35] or a conical shell [36] are not suitable for modeling of the discrete nature of the fabric yarn structure. In view of this limitation, in our analysis, the fabric is considered to be a discrete ensemble of interwoven yarns connected at the crossover points. The yarns are idealized as springs (linear or nonlinear), and the crossover points are assumed to be pin-jointed. This approach allows a more realistic description of deformation response such as orthotropic in-plane tensile properties of plain-weave fabrics. However, it should be noted that the effect of bending stiffness is neglected in the pin-joint model. In the present model, a mechanical system exhibits zero bending stiffness for loading in the transverse direction (out of the plane of the fabric). Although textile fabrics do have a finite bending stiffness, such an approximation appears to be quite reasonable considering that the polymeric fibers comprising the textile structure have a very low moment of inertia, and that the textile composites of interest in this study have a very low resin content.

For the model developed herein, the transverse displacement of the nodes that fall under the penetrator are set equal to the penetrator displacement at every time step. The displacements of the nodes at the clamp are set equal to zero. The displacements of the remaining nodes can be found using an equilibrium equation derived from a consideration of the deformation geometry. Upon writing an equilibrium equation for every node in the mesh, one can obtain a simultaneous system of nonlinear, coupled algebraic equations. In the present study, a modified Newton's method was used to solve this system of nonlinear equations. The roots are the out-of-plane displacements for every node in the mesh. Once these displacements are known under the force imparted onto the penetrator, the strains and stresses can be calculated, thereby solving the entire problem.

RESULTS AND DISCUSSION

Effect of Clamping Force on Penetration Resistance

Figure 3 shows the total amounts of drop-weight impact energy absorbed by fully penetrated 5-ply laminate specimens of Spectra 900 fabric-reinforced vinyl ester resin composite. The clamping forces ranged from 2 kN to 406 kN. The 2 kN force happened to be a typical level of maximum clamping force obtainable with the pneumatic fixture of drop-weight impact tester. Clamping forces higher than 2

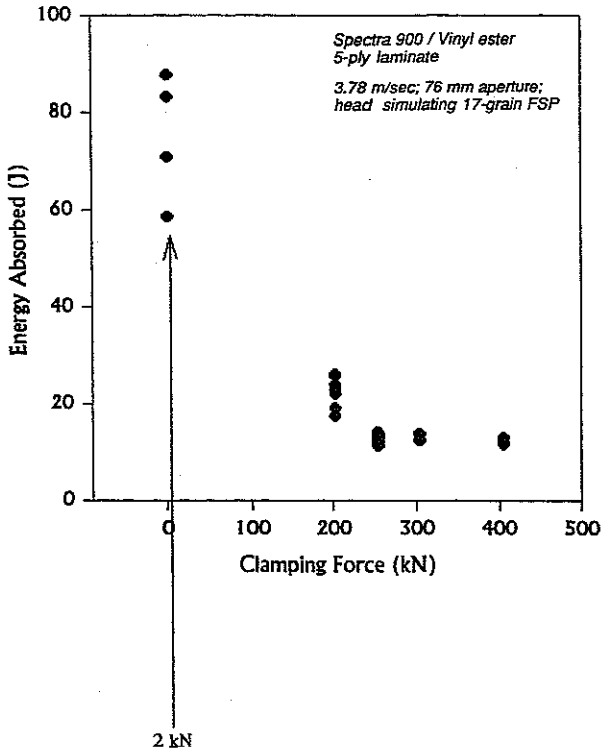

Figure 3. *Impact energy absorbed vs. clamping force for 5-ply laminates of Spectra 900® fabric-reinforced vinyl ester resin composite subjected to the impact mass of 12.3 Kg falling at the speed of 3.78 m/s.*

kN were obtained using the fixture described earlier (Figure 2). When the clamping force exceeded the level between 203 and 254 kN, the impact energy was found to be independent of clamping force, indicating that no specimen slippage occurred. Less scatter of data was also observed above the critical clamping force of 254 kN. Obviously the typical clamping force of 2 kN provided by commercially-available test fixture was not sufficient for the flexible version of armor-grade composite laminates. In fact, the average value of impact energy absorbed at the clamping force of 2 kN was about 4.5 times the value at 254 kN because of the specimen slippage (Figure 3).

Figure 4 shows light-transmission photographs of the Spectra fabric-reinforced composite specimens subjected to the drop-weight impact at the clamping pres-

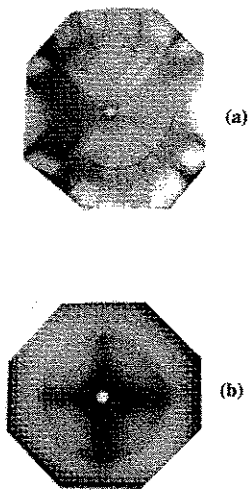

Figure 4. Light transmission photographs of fully penetrated 5-ply laminates of Spectra 900® fabric-reinforced vinyl ester resin composite at the clamping force of: (a) 2 kN, (b) 406 kN.

sures of 2 kN and 406 kN. For the purpose of examination, the 76.2 mm aperture boundary was traced on these plates. The plate damage extended well beyond the aperture boundary at the clamping force of 2 kN. On the other hand, the delamination, fiber straining, and other types of damage patterns were well contained within the aperture boundary at the clamping force of 406 kN, indicating no specimen slippage.

The calibration curves similar to that of Figure 3 were generated for each laminate system to determine the critical clamping forces needed to prevent the specimen slippage under the loading conditions of static puncture as well as drop-weight impact. The critical clamping forces required for static puncture loading were found to be slightly higher than those for drop-weight impact loading. All penetration testing was done at the clamping forces well above these critical levels. It should be noted that the aperture size and boundary conditions for the specimens used in this study were chosen rather arbitrarily. The boundary conditions encountered in actual applications such as protective vests and helmets may be different. More exhaustive investigations on the effects of boundary conditions are currently under way.

Effect of Resin Addition on Penetration Characteristics

In order to examine how the addition of matrix resin alters the penetration characteristics of woven fabrics, single ply specimens of dry Spectra fabric as well as Spectra fabric-reinforced composite lamina (25% by weight of resin) were tested side-by-side in both static puncture mode and drop-weight impact loading mode. Figure 5 shows the load-deflection response of Spectra fabric/vinylester resin and Spectra fabric/polyurethane resin composite laminae, while Figure 6 shows that of Spectra dry fabrics. The difference between the dry fabric and composite laminae was noted in the final failure mode. The composite laminae showed a sudden failure with one large drop of load. On the other hand, the failure of fabrics was associated with several load drops. Detailed observation during and after testing of the dry fabrics revealed that the numerous load drops in Figure 6 corresponded to (a) successive breaking of individual yarns along the periphery of the penetrating

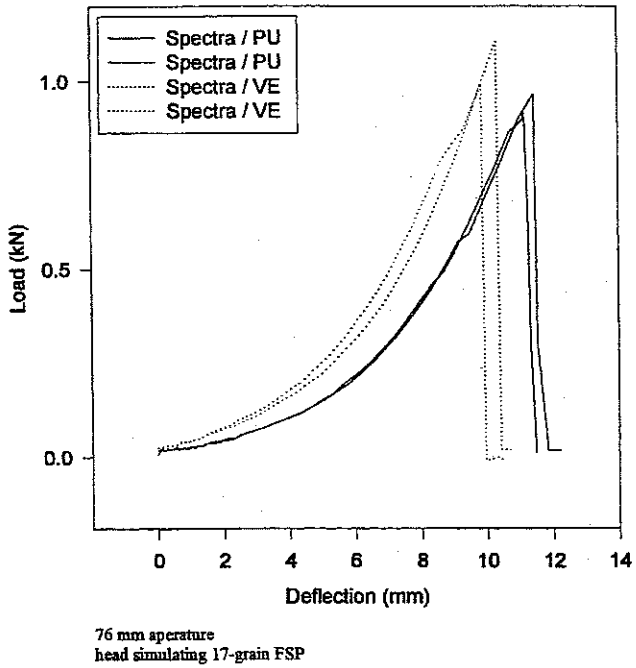

Figure 5. Load-deflection curves for single-ply composite laminae of Spectra 900® fabric-reinforced vinylester (VE) resin composite vs Spectra 900® fabric-reinforced polyurethane (PU) resin composite under static penetration loading at 0.000254 m/s.

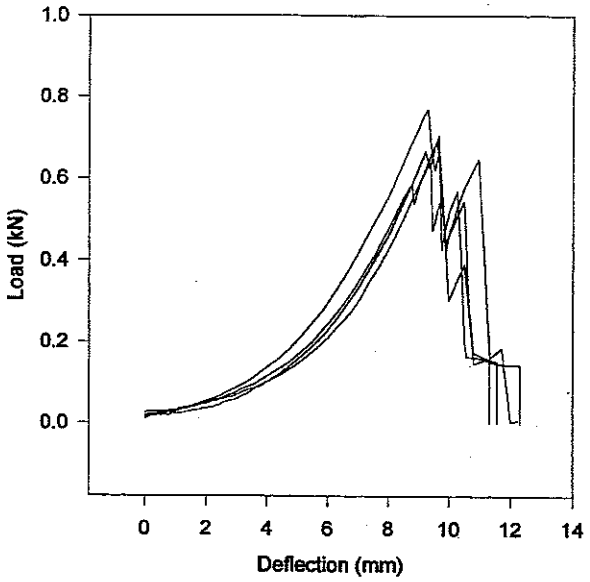

Figure 6. *Load deflection curves for single ply of Spectra 900® dry fabric under static penetration loading at 0.000254 m/s.*

head, and (b) the movement of yarns slipping off from the penetrator. Both of these events led to load drops in a sequential manner, since they resulted in a decrease in the number of yarns imparting force onto the penetrator.

In contrast to the case of dry fabric, the principal yarns in the composite, which face the penetrating head, failed to carry the load mostly through fracture due to the constraint of the resin matrix. The composites failed at a much higher load than the fabrics, because it would require more force to break many yarns simultaneously than to break them one or two at a time. Therefore, one effect of resin addition appeared to be coupling of the yarns so as to make the stress state more uniform and the failure process more sudden compared with the dry fabrics. Figures 7(a) and 7(b) show SEM micrographs of the damaged regions of dry fabric and composite laminae subjected to drop-weight impact loading, respectively. For the composite, a fully penetrated region consisted of approximately 2.75×4.31 yarns on the average. A fully penetrated region of the dry fabric consisted of only 2.00×3.94 yarns. This confirmed that some of the principal yarns in the dry fabrics slipped off from the penetrator during the penetration process without being broken. It should be

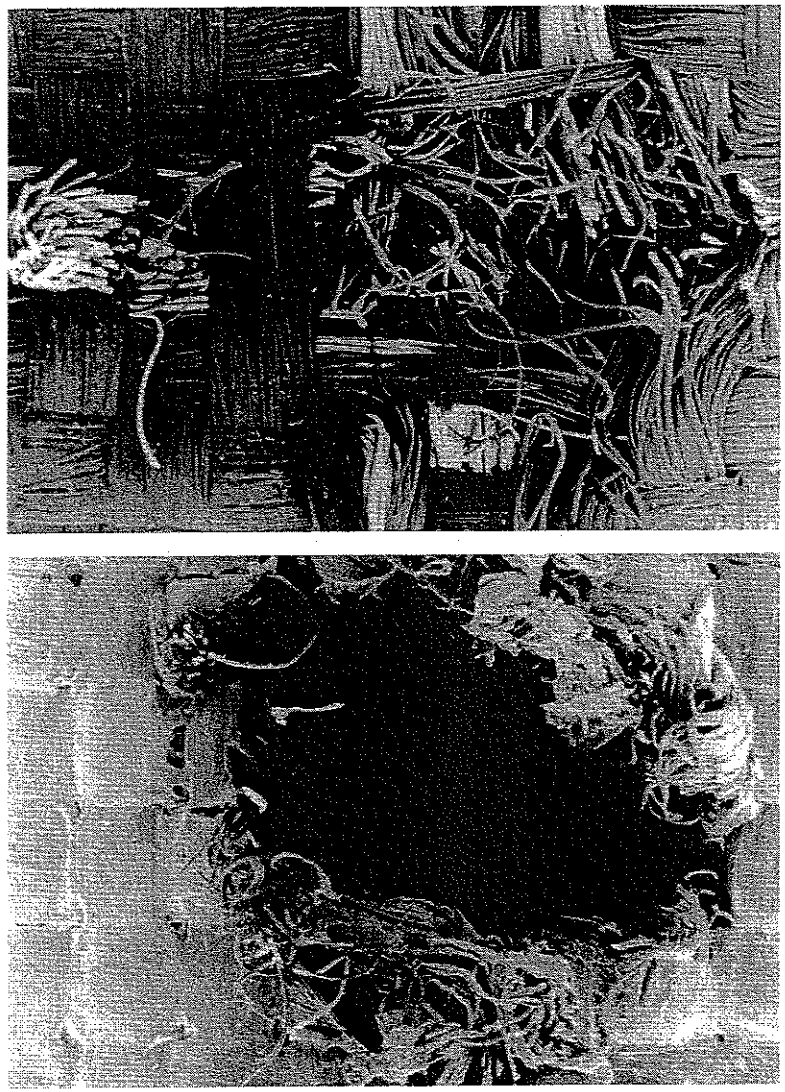

Figure 7. *SEM photographs of the failed region of (a) a single ply of Spectra 900® dry fabric, and (b) a single ply of Spectra 900® fabric reinforced polyurethane resin composite laminae, subjected to the impact mass of 12.3 Kg falling at the speed of 3.78 m/s.*

noted that the yarn deniers and penetrator diameters were the same in the two cases. Thus, due to yarn slippage, the fabrics engaged a smaller penetrator radius than did the composites.

Figure 7(a) clearly illustrates that, after fracturing, a yarn in the dry fabric sprang back (due to the unbalanced tensions) and unlaced itself through two adjacent yarns. The loss of tension in this yarn after fracture caused, in turn, decrimping of the surrounding yarns, thereby decreasing weave tightness in the vicinity of the penetrator. As the weave in the vicinity of the penetrator became more loose following further yarn failures, yarn mobility would increase and yarns would slip off from the penetrator. This type of phenomenon could not occur easily in the composites since the yarns were constrained to each other due to the presence of the resin matrix. As a result, the final failure processes in dry fabrics and composites became quite different. However, the degree of difference between the two cases may vary with the change of yarn denier, fiber type, fabric construction, the number of plies, penetrator geometry, and resin system. For example, impact-resistant fabrics with smaller denier yarns may have tighter weaves and may not be as susceptible to the movement of yarns. When yarn slippage occurred in the dry fabrics, the slipped yarns could not absorb as much energy as could the same yarns strained to failure in the composites.

The observation discussed so far was further quantified by counting the numbers of principal yarns broken by the penetrator in the specimens and relating them to the levels of impact energy absorbed. As shown in Table 1, the ratio of energy absorbed by the fabrics (as measured by integrating the load-deflection curves) to that of the composites was about 0.85, while the ratio of the number of broken yarns in the fabric to that of the composites was about 0.84. A clear correlation between these two parameters confirms that fiber straining is responsible for most of the energy absorption in penetration failure of textile fabrics and fabric-reinforced composites. Although the resin matrix itself did not absorb significant energy, it certainly did have an indirect effect on the energy absorption capacity of composites by influencing the number of yarns that were broken, as will be discussed later.

Penetration Failure Mechanisms

The penetrator geometry appeared to play a role in the yarn mobility of the dry fabrics. Detailed examination during and after penetration revealed that the tapered regions on the FSP were the locations of yarn slippage. With an advance of the penetrating head, some of the yarns that were parallel to the longer side of the FSP front face failed first, which corresponded to the first load drop in Figure 6. After further yarn failures and the corresponding decrimping and weave loosening, the remaining yarns parallel to the longer side of the front face were found to slide along the tapered region and eventually slip off from the penetrating head instead of being broken. The yarns that were parallel to the shorter dimension of the

Table 1. Energy absorbed vs. the number of broken yarns in single-ply of Spectra 900® fabric-reinforced composite laminae [(ve): vinylester matrix; (pu): polyurethane matrix] and single-ply of Spectra 900® dry fabrics subjected to the impact mass of 12.3 Kg falling at the speed of 3.78 m/s.

Spectra® 900 Composite Lamina		Spectra® 900 Dry Fabric	
Energy Absorbed (J)	Number of Broken Yarns	Energy Absorbed (J)	Number of Broken Yarns
3.45 (ve)	2.50 × 4.50	2.69	2.00 × 3.75
3.64 (ve)	3.50 × 4.25	2.65	2.00 × 4.25
3.51 (pu)	2.00 × 4.25	3.26	2.00 × 3.75
3.30 (pu)	3.00 × 4.25	3.19	2.00 × 4.00
Average: 3.48	Average: 2.75 × 4.31	Average: 2.95	Average: 2.00 × 3.94
Average ratio of number of broken yarns in dry fabrics over that of composite laminae			0.84
Average ratio of energy absorbed in dry fabrics over that of composite laminae			0.85

front face could not slip as easily since lateral movement along the inclined surfaces was more difficult in this orientation. As a result, the dimensions of failure regions in dry fabric were asymmetric (roughly 2.00 × 3.94 yarns). Since the addition of a resin suppressed decrimping action and resulting yarn slippage, the composites exhibited a more uniform failure region (roughly 2.75 × 4.31 yarns). A certain amount of yarn slippage must have occurred in the composite laminae since the dimensions of their failure regions were still asymmetric.

Having established the location of yarn slippage as being along the inclined surfaces of the penetrator, further discussion is necessary as to how the projectile shape in general will affect the yarn slippage and hence overall performance during the penetration process. As discussed earlier, Dent et al. [17] noted that blunt-nosed projectiles engaged and broke more yarns during penetration than did hemispherical penetrators. This observation was used to explain the lower critical velocity for penetration of panels impacted with projectiles of the latter shape. It is interesting to note that (a) blunt-nosed projectiles have no tapering, (b) the inclined surfaces of the FSP constitute tapering at a constant angle, and (c) hemispherical projectiles are tapered continuously. Since tapered penetrators induce more yarn slippage than do blunt-nosed penetrators due to the ability of the yarns to slide along the inclined surfaces in the former case, tapered penetrators should penetrate the fabric more easily. From the results presented earlier, it appears that the penetration resistance of single-ply laminae show less dependence on the degree of penetrator tapering than do dry fabrics due to the constraint of the resin matrix.

Numerical Modeling

Our newly formulated numerical model was utilized to examine the effect of penetrator radius on the energy absorption capacity of a given fabric. The results of numerical simulation are shown in Figure 8. As expected, the larger the radius of the penetrator, the larger is the force imparted onto it by the fabric. The areas under the curves of Figure 8 correspond to the energy absorbed by the fabric which, in a situation where the penetrator velocity was not machine-driven (such as in low-velocity, drop-weight impact), would correspond to the loss of penetrator kinetic energy. As a consequence, a penetrator with a larger diameter is expected to slow down more quickly in a low-velocity impact situation than the case of a slender penetrator, assuming equal impactor masses.

The described predictions of the numerical model are consistent with the experimental results of drop-weight impact testing discussed earlier. As seen in Table 1, a greater number of yarns were broken during the penetration of composite laminae than the case of dry fabrics which allow more yarn slippage. The results clearly indicate that the composite laminae engage a larger effective penetrator radius than did the dry fabrics. This trend became more apparent after yarn slippage since, before the initial load drops, the fabrics and composites engaged roughly the same number of yarns. The composites absorbed a correspondingly larger amount

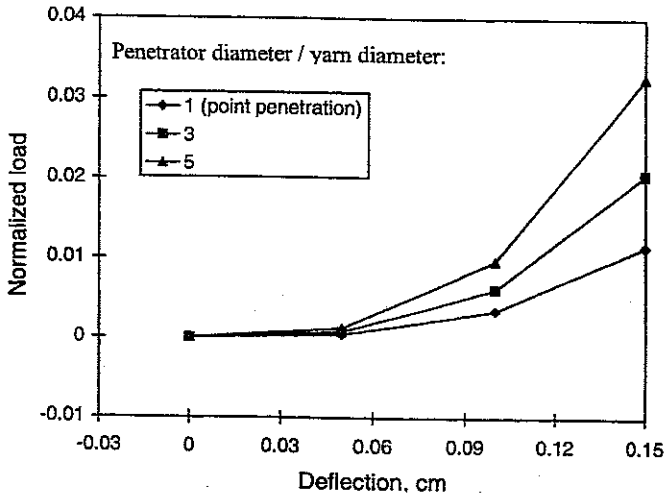

Figure 8. *Numerical modeling of the effect of penetrator radius on the normalized load-deflection response of a plain-weave fabric.*

of penetration energy than did the fabrics, confirming the general relationship between the penetrator radius and the energy absorption capacity which is predicted by the numerical model at a constant velocity of penetrator.

Ballistic Limit and Penetration Energy

In this study, a series of ballistic tests for composite panels were performed at various levels of striking velocity to estimate the ballistic limit velocity, i.e., a threshold velocity for full perforation. Ballistic tests were done using either hemispherical projectile of tungsten carbide ball or FSP projectile with a rectangular front face followed by two inclined planes tapering into the full penetrator diameter (Figure 1). Clamping forces for test panels were well above the critical levels defined earlier under the loading conditions of static puncture as well as drop-weight impact. As illustrated in Figure 9 that deals with two specific cases of Spectra fabric-reinforced composite and aramid fabric-reinforced composite, the impact of tungsten carbide ball at various levels of striking velocity led to either full perforation or no/partial perforation with rebound action. Graphic plot allowed the estimation of the ballistic limit velocity, V_{50}, which was defined as the highest striking velocity, V_s, where the residual or rebound velocity, V_r, equals zero.

Along with this direct way of defining V_{50} from the graphic plots, an indirect way of estimating V_{50} was incorporated in the evaluation using the following relationship for fully perforated specimens:

$$1/2mV_r^2 = 1/2mV_s^2 - 1/2m(V_{50})^2$$
$$V_{50} = (V_s^2 - V_r^2)^{1/2} \text{ for } V_r > 0$$

where V_s is striking velocity, V_r is residual velocity, and m is the mass of the projectile. The relationship assumes non-deformable penetrator and the conservation of energy. The V_{50} values calculated using the above equation were very close to those obtained directly from a multiple number of tests at various levels of V_s.

Relying on the same assumptions of non-deformable penetrator and the conservation of energy, the amount of kinetic energy absorption for full penetration, E^*, was estimated from V_{50} using the relationship of $E^* = 1/2\ m(V_{50})^2 = 1/2\ m(V_s^2 - V_r^2)$. The results allowed fair comparisons of penetration resistance of materials in terms of energy absorption which is solely dependent on projectile mass and independent of projectile composition, as revealed in our concurrent study of ballistic impact performance of other structural materials [37]. For the current study, V_{50} and E^* were estimated respectively as a function of target thickness for Kevlar aramid fabric-reinforced phenolic-polyvinylbutyral resin composites. The results will be discussed in a later section of this paper.

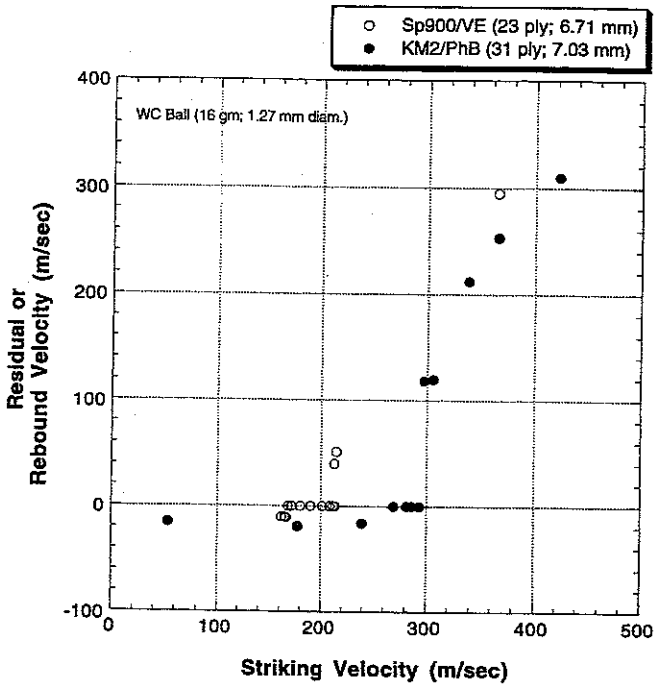

Figure 9. The relationship between the residual velocity vs. striking velocity for the 23-ply laminates of Spectra 900® fabric-reinforced vinylester resin composite (6.71 mm thick) and 31-ply laminates of Kevlar KM2® fabric-reinforced phenolic-polyvinylbutyral resin composites subjected to the impact of tungsten carbide ball (16 g, 12.7 mm diam.).

Multi-Ply Composite Laminates with Different Resin Matrices

Having developed a basic understanding of penetration processes of single-ply composite laminae, the next topic for investigation was the response of 5-ply composite laminates. For this investigation, Spectra 900 fabric-reinforced composite laminates with vinylester and polyurethane resin matrices were tested in the following loading modes: static puncture (0.000254 m/s); low-velocity drop-weight impact (12.3 Kg, 3.78 m/s); and ballistic impact (1.1 g, 200-250 m/s). The same FSP geometry of the penetrator was used in all tests. The above tests allowed comparative evaluation of the energy absorbed for the penetration of two composites with different matrix stiffness over a relatively wide range of strain rates. In the cases of static puncture and low-velocity impact loading, the amounts of energy

absorption were determined using the average values of the area under the load-deflection curve (for three to six specimens). For ballistic impact tests, the amounts of energy absorption were estimated from the relationship of $E^* = 1/2m(V_{50})^2 = 1/2m(V_s^2 - V_r^2)$ and determined by testing of about ten specimens.

As shown in Table 2, the vinylester resin matrix composites outperformed the polyurethane matrix composites by 14 to 17% over the entire range of strain rates. Despite unusually high values of energy absorption observed for slow penetration under static loading, the ratios of energy absorbed for the penetration of vinylester resin matrix composites to those of the polyurethane matrix composites appeared to be independent of strain rate. Unusually high values of energy absorption observed for slow penetration under static loading may result from the fact that the penetrator velocity was machine-driven, in contrast to the case of ballistic or drop-weight impact in which the penetrator decelerates resulting in variable penetration velocity. Although the data suggest that material comparisons carried out at any strain rate result in the same trends in performance for these particular materials, it is recognized that this may not be the case for all material systems when time-dependent failure processes are involved.

As discussed earlier, the composite lamina failed at a much higher load than the corresponding dry fabric under static penetration loading, because it would re-

Table 2. Energy absorption for full perforation of 5-ply laminates of Spectra fabric-reinforced composite with vinylester and polyurethane resin matrices.

	Energy Absorption (J) for Full Penetration		
	Static Puncture (0.00025 m/s)	**Drop Weight Impact (3.78 m/s; 12.3 Kg)**	**Ballistic Impact (220–260 m/s; 1.1 g)**
Spectra® 900/ Vinylester 5-ply composite laminate	31.9	16.9	35.63
	26.4	16.5	32.64
	26.3	16.3	32.63
		15.9	28.52
			20.95
Ave.	28.2	16.4	30.07
Spectra® 900/ polyurethane 5-ply composite laminate	26.9	15.7	32.92
	25.4	14.7	27.93
	25.2	14.7	26.18
	22.9	14.4	22.46
	22.3	13.4	20.27
	21.4	13.1	
Ave.	24.0	14.3	25.95
Ratio	1.17	1.14	1.16

quire more force to break many yarns simultaneously than to break them one or two at a time. In accordance with the above contention, the ratio of energy absorbed by the fabrics to that of the composite laminae was found to be correlated well with the ratio of the number of broken yarns under drop-weight impact loading (Table 1). Apparently, fiber straining is responsible for most of the energy absorption during the penetration failure of armor-grade composites as in the case of dry fabrics. However, the resin matrix did have an indirect effect on the energy absorption capacity of composites by reducing the mobility of yarns and thereby increasing the number of yarns broken.

Within this context, a possible explanation for the superior performance of the vinylester matrix composite laminates under ballistic impact (Table 2) should come from the differences in yarn mobility. In fact, the dependence of yarn mobility of the composite laminates on the resin matrix properties could be confirmed by measuring the number of broken yarns in failed regions of individual plies. As shown in Table 3, the average number of broken yarns was distinctly higher for vinylester matrix composites (3.47 × 3.87 yarns) than for polyurethane matrix composites (2.70 × 3.20 yarns). The number of broken yarns appeared to be constant throughout the thickness for both composite laminates. After normalizing with the values of total number of broken yarns throughout the laminate thickness in both warp and filling directions, the level of ballistic impact energy

Table 3. Energy absorbed vs. the number of broken yarns in individual plies [(1) : Ply #1 facing the projectile] for 5-ply laminates of Spectra 900® fabric-reinforced composite with vinylester and polyurethane resin matrices subjected to the fragment-simulating projectile of 1.1 grams at the speed of 220 to 260 m/s.

Spectra® 900/Vinylester 5-Ply Composite Laminate		Spectra® 900/Polyurethane 5-Ply Dry Fabric	
Energy Absorbed (J)	Number of Broken Yarns in Each Ply (ply #)	Energy Absorbed (J)	Number of Broken Yarns in each Ply (ply #)
32.64	3.00 × 3.50 (1) 3.50 × 3.80 (2) 3.50 × 4.10 (3) 3.50 × 3.80 (4) 3.80 × 4.30 (5) Average 3.47 × 3.87	26.18	2.00 × 4.00 (1) 3.00 × 2.00 (2) 2.50 × 3.00 (3) 3.00 × 3.00 (4) 3.00 × 4.00 (5) Average 2.70 × 3.20

	Ratio of Energy Absorbed to the Number of Broken Yarns
Spectra® 900/vinylester 5-ply composite laminate	0.89 (J)
Spectra® 500/polyurethane 5-ply composite laminate	0.89 (J)

absorbed per each broken yarn was found to be 0.89 which is independent of matrix composition.

The results discussed so far indicate that vinylester matrix composites outperform polyurethane matrix composites simply because more fibers are broken in the former. This observation is consistent with our earlier speculation [1] that resin stiffness may play a primary role in controlling the ballistic impact resistance of Spectra fabric-reinforced composite laminates. A stiffer resin couples the yarns more effectively and prevents the yarn movement to a greater degree. The reduction of yarn mobility, in turn, forces the penetrator to engage and break more yarns thereby resulting in an increased energy absorption and overall performance of the panel.

However, it is premature to assume the validity of the described failure criterion in the case of thicker composite laminates without further experimental evidence. Fiber mobility due to the presence of resin is considered to be one of many factors that possibly affect the impact resistance. For instance, localized Hertzian failure along the periphery of the penetrator may also influence the penetration resistance of multi-ply composites due to the increasing bending stiffness with increasing laminate thickness. In this situation, the delamination behavior might influence overall performance of composite laminates. These factors and others are the subjects of ongoing studies which led to our initial assessment of the effect of laminate thickness on the ballistic limit.

Effect of Laminate Thickness on Ballistic Limit

The effect of laminate thickness on the ballistic limit of aramid fabric-reinforced composites was examined to further assess the relationship between fiber straining and fiber mobility in controlling energy absorption mechanisms. Our concurrent study of ballistic impact performance of other structural materials [37] demonstrated that the nature of energy absorption mechanisms is related to the exponent value of a power law correlation for ballistic limit velocity (V_{50}) versus target panel thickness. For ductile monolithic materials such as polycarbonate and aluminum, penetration failure was found to start with "local yielding" and "dishing/bulging" which developed into tensile failure of rear surface producing practically no fragments. The values of the exponent depicting the thickness dependence of V_{50} were found to be around 0.5 for both materials, since the kinetic energy absorbed at the threshold velocity for full perforation, $1/2m(V_{50})^2$, is linearly proportional to the thickness. The observed linearity indicates that the amount of kinetic energy absorption for full penetration of ductile monolithic materials is governed by the tensile fracture energy of materials through the thickness. With a given fracture energy of materials, the increase of target thickness (i.e. cross-section of panel) should result in a linearly proportional change in the amount of kinetic energy absorption for full penetration.

In contrast to polycarbonate or aluminum, structural-grade composites (fiber volume of about 55%) of graphite fiber-reinforced epoxy resin exhibited complex failure modes of matrix/interface cracks and delamination along with fiber fracture creating a great number of fragments. These three-dimensional modes of crack propagation with fragmentation and resulting mass loss provided additional mechanisms of energy absorption during the penetration failure of composites. As a result, the exponent depicting the thickness dependence of V_{50} was 0.66 to 0.67 (instead of 0.5) in the case of graphite fiber-epoxy resin composites, although the overall level of V_{50} for graphite fiber composites remained lower than that of polycarbonate or aluminum at given panel thickness. As expected, the kinetic energy for full perforation, $1/2m(V_{50})^2$, became proportional to the thickness in non-linear fashion with the exponent of 1.34, indicating a steady rise of penetration energy required per unit thickness with the increase of panel thickness.

The current experimental study showed that, in terms of penetration failure modes, the armor-grade fabric-reinforced resin composites share certain common features with both ductile monolithic materials and structural-grade fiber composites. As in the case of polycarbonate or aluminum, the penetration failure of the armor-grade composites reinforced with Spectra or aramid fabric was accompanied by ductile deformation of reinforcement in "bulging" mode, especially when the composite laminates remain relatively thin (less than 3 mm). At the point of full perforation, ductile deformation of fabric reinforcement developed clearly into tensile failure (i.e. tear) of rear surface. However, tensile failure mode of armor-grade fabric-reinforced composites was different from that of ductile monolithic materials in the fact that the energy absorption capacity is dependent on not only fracture energy but also the mobility of yarns. As discussed earlier, the yarn mobility of the composite laminates affects the number of broken yarns thereby influencing a critical level of energy absorption for full perforation.

In addition to the above-described mode of tensile failure, the penetration failure of aramid or Spectra fabric-reinforced composites involved matrix/interface cracks and delamination, as in the case of structural-grade composites of graphite fiber-reinforced epoxy resin. But the measurement of test panel weights before and after ballistic testing confirmed that these failure modes occurred without creating an appreciable number of fragments, in contrast to the case of structural-grade composites. Virtually no mass loss was observed even in relatively thick panels (3–7 mm thick) of aramid fabric-reinforced composites. The observed modes of penetration failure did in turn influence the thickness dependence of ballistic limit velocity, V_{50}, or the kinetic energy absorbed at the threshold velocity for full perforation, $1/2m(V_{50})^2$, of armor-grade composites (Figure 10 and Figure 11).

Up to the laminate thickness of 3 mm, the exponent depicting the thickness dependence of V_{50} was 0.42 for Kevlar KM2 aramid fabric-reinforced composites. The values of $1/2m(V_{50})^2$ were dependent on the laminate thickness with the

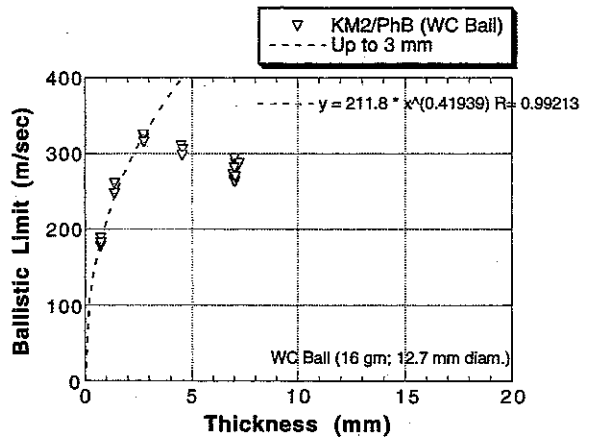

Figure 10. Threshold velocity for full perforation, V_{50}, for Kevlar KM2® fabric-reinforced phenolic-polyvinylbutyral resin composite panels of various thicknesses subjected to ballistic impact of tungsten carbide ball (16 g, 12.7 mm diam.).

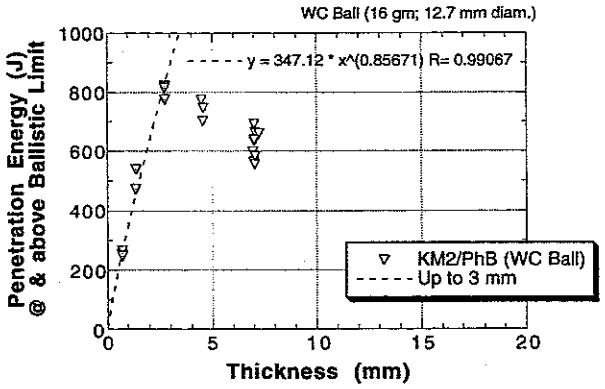

Figure 11. Amount of kinetic energy absorption for full penetration, E, for Kevlar KM2® fabric-reinforced phenolic-polyvinylbutyral resin composite panels of various thicknesses subjected to ballistic impact of steel ball (16 g, 12.7 mm diam.).*

power-law exponent of 0.86. Apparently, the thickness dependence of the kinetic energy for full perforation of armor-grade fabric-reinforced composites was close to the case of ductile monolithic materials such as polycarbonate or aluminum but in less linear fashion. The deviation from the linearity probably reflects a unique mode of tensile failure of armor-grade composites in which a critical level of kinetic energy for full perforation is lowered by the mobility of yarns. If the energy absorption process is solely dependent on tensile failure of yarns without any influence of yarn mobility, the thickness dependence of $1/2m(V_{50})^2$ should be linear (exponent of 1) as in the case of polycarbonate or aluminum.

When the panel thickness exceeded 3 mm, both V_{50} and $1/2m(V_{50})^2$ for aramid fabric-reinforced composites remained the same or decreased slightly with increasing thickness. Although the final conclusion is too early to draw at present, this behavior could be attributed to the transition of deformation mode. In fact, it was observed that, when the laminate thickness exceeded 3 mm, the armor-grade composite panels became rigid (no longer bendable by hand) and bulging of rear surface due to ballistic impact became less pronounced. The observation indicates that the penetration failure of armor-grade fabric-reinforced composites is no longer dominated by "in-plane membrane tension" above a critical level of laminate thickness which is around 3 mm in the case of Kevlar KM2 fabric-reinforced phenolic-polyvinylbutyral resin. Further study is planned to assess the ballistic performance of aramid and Spectra fabric-reinforced composites with the thickness range beyond 7 mm, and to assess the roles of delamination and localized Hertzian failure along the periphery of the penetrator when "plate bending" becomes a prevalent mode of deformation.

CONCLUSIONS

In this study, the mechanisms of penetration failure were examined for the armor-grade composites reinforced with Spectra or aramid fabric under static puncture, low-velocity impact as well as ballistic impact loading conditions. The failure modes of dry fabrics, composite laminae, and composite laminates were compared to gain a fundamental understanding of the deformation and failure processes involved. The following conclusions could be drawn:

1. High clamping pressures are required to ensure no slippage of flexible armor-grade composite specimens under in-plane membrane tension induced by transverse loading. When the clamping force exceeds a critical level (between 203 kN and 254 kN under drop-weight impact), the impact energy becomes independent of clamping force.
2. Failure of dry fabrics consists of the successive fracture of individual yarns along the periphery of the penetrating head as well as the movement of yarns slipping off from the penetrator. In contrast, the principal yarns in the composite, which face the penetrating head, fail to carry the load mostly through fracture due to the constraint of the resin matrix and the decreased yarn mobility.
3. Since more yarns are broken in the composites, the composites absorb more energy than the fabrics. The ratio of broken yarns in the fabrics to that of the composites correlates quite well with the corresponding ratio of energy absorbed, confirming that fiber straining is responsible for most of the energy absorption in penetration failure.
4. Numerical modeling verifies that larger penetrator radii produce greater energy absorption during the penetration of plain-weave fabrics due to the engagement of more yarns. This trend can be related to the difference in performance between dry fabrics and composite laminae. Yarn slippage in the fabrics results in a smaller effective penetrator radius leading to a decrease in energy absorption capacity with equal penetrator masses.
5. Although the resin matrix itself does not absorb significant amounts of energy, it certainly has an indirect effect on the energy absorption capacity of composites by influencing the number of yarns broken. Stiffer resin matrix prevents the yarn movement to a greater degree and thereby forces the penetrator to engage and break more yarns.
6. The penetration failure of the armor-grade composites is accompanied by ductile deformation of fabric reinforcement developing into tensile failure of rear surface, as in the case of ductile monolithic materials such as polycarbonate or aluminum. The penetration failure also involves matrix/interface cracking and delamination but without creating an appreciable number of fragments, in contrast to the case of structural-grade fiber composites.
7. Up to the thickness of 3 mm, the dependence of the kinetic energy for full perforation of armor-grade composites on the laminate thickness is close to the case of ductile monolithic materials such as polycarbonate or aluminum but in less linear fashion. The deviation from the linearity probably reflects a unique mode of tensile failure of armor-grade composites in which a critical level of kinetic energy for full perforation is lowered by the mobility of yarns.

ACKNOWLEDGMENTS

We sincerely appreciate continuing support for this research work from the Air Vehicles Directorate of Air Force Research Laboratory (Wright-Patterson AFB) and Army Soldier Systems Command RD&E Center (Natick, MA). We are also grateful to Dr. Ashok Bhatnagar and the late Dr. Hae-Won Chang at AlliedSignal Inc. for providing the materials and all necessary information.

REFERENCES

1. Lee, B. L., Song, J. W. and Ward, J. E., "Failure of Spectra® Polyethylene Fiber-Reinforced Composites under Ballistic Impact Loading," *J. Composite Materials*, v. 28 (13), 1202–1226 (1994).
2. Prevorsek, D. C., Kwon, Y. D. and Chin, H. B. "Analysis of the Temperature Rise in the Projectile

and Extended Chain Polyethylene Fiber Composite Armor during Ballistic Impact and Penetration," *Polymer Engineering and Science*, v. 34, 141–52 (1994).

3. Zhu, G., Goldsmith, W. and Dharan, C. K. H., "Penetration of Laminated Kevlar by Projectiles. I. Experimental Investigation," *Int. J. Solids. Struct.*, v. 29 (4), 399–420 (1992).
4. Zhu, G., Goldsmith, W. and Dharan, C. K. H., "Penetration of Laminated Kevlar by Projectiles. II. Analytical Model," *Int. J. Solids Struct.*, v. 29 (4), 421–436 (1992).
5. Schuman, T. L., "S2000 Ballistic Hardened C3I Shelter," *Proc. of the 24th SAMPE Int'l Tech. Conf.*, T280–T290 (1992).
6. Segal, C. L., "High-Performance Organic Fibers, Fabrics and Composites for Soft and Hard Armor Applications," *Proc. of the 23rd SAMPE Int'l Tech. Conf.*, 651–660 (1991).
7. Riewald, P. G., Folgar, F., Yang, H. H. and Shaughnessy, W. F., "Lightweight Helmet from A New Aramid Fiber," *Proc. of the 23rd SAMPE Int'l Tech. Conf.*, 684–695 (1991).
8. Thomas, T. S., "Facets of a Lightweight Armor System Design," *Proc. of the 22rd SAMPE Int'l Tech. Conf.*, 304–318 (1990).
9. Prevorsek, D. C. and Chin, H. B., "Development of a Light Weight Spectra Helmet," Phase I Interim Technical Report from AlliedSignal Inc. to U.S. Army Natick RD&E Center, Natick, MA (DAAK60-87-C-0089/D) (1988).
10. Song, J. W. and Egglestone, G. T., "Investigation of the PVB/PF Ratios on the Crosslinking and Ballistic Properties in Glass and Aramid Fiber Laminate Systems," *Proc. of the 19th SAMPE Int'l Tech. Conf.*, 108–119 (1987).
11. Donovan, J. G., Kirkwood, B. and Figucia, F., "Development of Lower Cost Ballistic Protection," U.S. Army Natick RD&E Center (Natick, MA) Technical Report Natick/TR-85/019L (1985).
12. Lin, L. C., Bhatnagar, A. and Chang, H. W., "Ballistic Energy Absorption of Composites," *Proc. of the 22rd SAMPE Int'l Tech. Conf.*, 1–13 (1990).
13. Smith J. C., Blandford J. M. and Schiefer H. F. "Stress-Strain Relationships in Yarns Subjected to Rapid Impact Loading: Part VI. Velocities of Strain Waves Resulting from Impact," *Text. Res. J.*, v. 30 (10), 752 (1960).
14. Smith J. C., Blandford, J. M. and Towne, K. M., "Stress-Strain Relationships in Yarns Subjected to Rapid Impact Loading: Part VIII. Shock Waves, Limiting Breaking Velocities, and Critical Velocities," *Text. Res. J.*, v. 32 (1), 67 (1962).
15. Roylance, D, Wilde, A. and Tocci G., "Ballistic Impact of Textile Structures," *Text. Res. J.*, v. 43, 34–41 (1973).
16. Cunniff, P. M., "An Analysis of the System Effects in Woven Fabric under Ballistic Impact," *Text. Res. J.*, v. 62 (9), 495–509 (1992).
17. Dent, R. W. and Donovan, J. G., "Projectile Impact with Flexible Armor—An Improved Model," U.S. Army Natick RD&E Center (Natick, MA) Technical Report Natick/TR-86/044L (1986).
18. Hsieh, C. Y., Mount, A., Jang, B. Z. and Zee, R. H., "Response of Polymer Composites to High and Low Velocity Impact," *Proc. of the 22nd SAMPE Int'l Tech. Conf.*, 14–27 (1990).
19. Critescu, N., Malvern, L. E. and Sierakowski, R. L., "Failure Mechanisms in Composite Plates Impacted by Blunt-Ended Penetrators," *Foreign Object Impact Damage to Composites, ASTM STP #568*, 159–172, ASTM, Philadelphia, PA (1975).
20. Cairs, D. S. and Lagace, P. A., "Transient Response of Graphite/Epoxy and Kevlar/Epoxy Laminates Subjected to Impact," *AIAA Journal*, v. 27 (11), 1590–1596 (1989).
21. Lin, J. L. and Lee, Y. J., "Use of Statical Indentation Laws in the Impact Analysis of Composite Laminated Plates and Shells," *J. Appl. Mech.*, v. 57, 787–789 (1990).
22. Lee, S. M. and Zahuta, P., "Instrumented Impact and Static Indentation of Composites," *J. Composite Materials*, v. 25 (2), 204–222 (1991).
23. Cantwell, W. J. and Morton, J., "Impact Perforation of Carbon Fibre Reinforced Plastic," *Composites Science and Technology*, v. 38, 119–141 (1990).
24. Walters, W. and Scott, B. R., "High Velocity Penetration of Kevlar Reinforced Laminate," *Proc. of the 22nd SAMPE Int'l Tech. Conf.*, 1078–1091 (1990).

25. Lee, S. W. R. and Sun, C. T., "Ballistic Limit Prediction of Composite Laminates by a Quasi-Static Penetration Model," *Proc. of the 24th SAMPE Int'l Tech. Conf.*, T497–T511 (1992).
26. Scott, B. R., "Cavity Expansion Theory Applied to Thick Kevlar Reinforced Composites," *Proc. of the 24th SAMPE Int'l Tech. Conf.*, T512–T523 (1992).
27. Choi, H. Y. and Chang, F. K., "Model for Predicting Damage in Graphite/Epoxy Laminated Composites Resulting from Low-Velocity Point Impact," *J. Composite Materials*, v. 26 (14), 2134–2169 (1992).
28. Jih, C. J. and Sun, C. T., "Prediction of Delamination in Composite Laminates Subjected to Low Velocity Impact," *J. Composite Materials*, v. 27 (7), 684–701 (1993).
29. Mittal, R. K. and Khalili, M. R., "Analysis of Impact of a Moving Body on an Orthotropic Elastic Plate," *AIAA Journal*, v. 32 (4), 850–856 (1994).
30. Florence A. L, "Interaction of Projectiles and Composite Armor, Part II," U.S. Army Materials and Mechanics Research Center (Watertown, MA) Technical Report AMMRC-CR-69-15 (1969).
31. Rajendran, A. M. and Kroupa, J. L., "Impact Damage Model for Ceramic Materials," *J. Applied Physics*, v. 66, 3560–3565 (1989).
32. Rosenberg, Z., Brar, N. S. and Bless, S. J., "Dynamic High-Pressure Properties of Al-N Ceramic as Determined by Flyer Plate Impact," *J. Applied Physics*, v. 70, 167–171 (1991).
33. "Standard Test Methods for Impact Resistance of Flat, Rigid Plastic Specimens by Means of a Tup (Falling Weight)," *American Society of Testing Materials (ASTM) Test Specification Designation D 3029-93*.
34. "Standard Test Methods for Impact Resistance of Flat, Rigid Plastic Specimens by Means of a Striker Impacted by a Falling Weight (Gardner Impact)," *American Society of Testing Materials (ASTM) Test Specification Designation D 5420-93*.
35. Lynch, D. F., "Dynamic Response of a Constrained Fibrous System Subjected to Transverse Impact Part II A Mechanical Model," Army Materials and Mechanics Research Center (Watertown, MA) Technical Report AMMRC TR-70-16 (1970).
36. Vinson, J. R. and Zukas, J. A., "On the Ballistic Impact of Textile Armor," *J. Appl. Mech.*, v. 42, 263–268 (1975).
37. Lee, B. L., Patts, H. M. and Mayer, A. H., "Penetration Failure of Fiber Composites vs. Monolithic Ductile Materials under Ballistic Impact," *Proc. of the 14th Tech. Conf. of Amer. Soc. for Composites*, 771–781, Dayton, OH (1999).